



HAL
open science

Real-time benchtop NMR spectroscopy for the online monitoring of sucrose hydrolysis

Alper Soyler, Dylan Bouillaud, Jonathan Farjon, Patrick Giraudeau, Mecit H Oztop

► **To cite this version:**

Alper Soyler, Dylan Bouillaud, Jonathan Farjon, Patrick Giraudeau, Mecit H Oztop. Real-time benchtop NMR spectroscopy for the online monitoring of sucrose hydrolysis. *LWT - Food Science and Technology*, 2020, 118, pp.108832. hal-02999920

HAL Id: hal-02999920

<https://hal.science/hal-02999920>

Submitted on 20 Nov 2020

HAL is a multi-disciplinary open access archive for the deposit and dissemination of scientific research documents, whether they are published or not. The documents may come from teaching and research institutions in France or abroad, or from public or private research centers.

L'archive ouverte pluridisciplinaire **HAL**, est destinée au dépôt et à la diffusion de documents scientifiques de niveau recherche, publiés ou non, émanant des établissements d'enseignement et de recherche français ou étrangers, des laboratoires publics ou privés.

Real-time benchtop NMR spectroscopy for the online monitoring of sucrose hydrolysis

Alper Soyler¹, Dylan Bouillaud², Jonathan Farjon², Patrick Giraudeau^{2,3*}, Mecit H. Oztop^{1*}

¹Department of Food Engineering, Middle East Technical University, Ankara, Turkey

²Université de Nantes, CNRS, CEISAM UMR 6230, Nantes, France

³Institut Universitaire de France, Paris, France

Corresponding Authors*:

e-mail: patrick.giraudeau@univ-nantes.fr

e-mail: mecit@metu.edu.tr

1 **ABSTRACT**

2 The online monitoring of chemical reactions by using benchtop Nuclear Magnetic
3 Resonance (NMR) spectroscopy has become increasingly attractive for the past few
4 years. The use of quantitative online NMR spectroscopy is a promising alternative to
5 traditional analytical methods with its rapid, quantitative and non-invasive nature that
6 makes it applicable to complex and diverse biochemical mixtures like food systems. In
7 this study, sucrose hydrolysis by invertase was chosen as a model reaction for online
8 monitoring. Rather than conventional NMR spectroscopy experiments that rely on the
9 use of deuterated water, the benchtop setting allows working in protonated solvents,
10 and tailored water suppression techniques were used to make quantification more
11 accurate. For the hydrolysis reaction, a 10% sucrose solution was hydrolyzed. The
12 kinetic constants determined by the fractional conversion model were comparable to
13 the results obtained in other studies. Quantitative online NMR spectroscopy is seen as
14 a promising tool for monitoring food processes in a continuous mode ~~and could be~~
15 ~~applied to different reactions like lactose free milk production, corn syrup production~~
16 ~~and hydrolysis of triglycerides.~~

Commenté [PG1]: you said in the response that this sentence was removed!

17

18 **Keywords:** Benchtop NMR spectroscopy, sucrose, invertase, flow NMR, online
19 monitoring, food applications

20

21 INTRODUCTION

22 Nuclear magnetic resonance (NMR) spectroscopy is one of the most common
23 techniques used by both chemists and biochemists to identify molecular structures as
24 well as to study the progress of chemical reactions (Marcone et al. 2013). NMR
25 spectroscopy has several advantages over commonly used analytical techniques like
26 high pressure liquid chromatography (HPLC), Raman spectroscopy, mass spectroscopy
27 (MS), gas chromatography (GC). NMR spectroscopy allows non-destructive,
28 quantitative analysis of liquid and solid samples requiring very small sample volumes.
29 It is also characterized by a short analysis time and a high reproducibility (Kumar et al.
30 2015). Due to the fact that many foods contain organic compounds, with protons
31 originating, e.g., from water, fat, carbohydrates, and proteins; proton NMR has become
32 the most common type of NMR to determine these abundant food components. Its non-
33 destructive and non-invasive nature has made NMR spectroscopy very popular in the
34 fields of food chemistry, food microbiology and food packaging (Pentimalli et al. 2000;
35 Nestor et al. 2010; Picone et al. 2011). The most studied areas are water/moisture
36 contents, lipid content, adulteration and authentication of foods (Keeton et al. 2003;
37 Chen et al. 2010; Hu et al. 2017; Gouilleux et al. 2018).

38 Despite the fact that NMR instruments date back to 1940s, because of its high capital
39 cost, operating expenditures, size and infrastructure needs, NMR found its place in food
40 research and industry after the first benchtop NMR relaxometry instrument was
41 introduced by Bruker in 1973. Although benchtop relaxometry instruments have been
42 in use in food research over 40 years, benchtop NMR spectrometers are very recent and
43 their potential in food industry is largely unexplored (Blümich and Singh 2018).
44 Benchtop NMR spectrometers can be used for process control purposes either by
45 online-monitoring in a flow cell or in an NMR tube (Dalitz et al. 2012; Meyer et al.

46 2016).

47 Quantitative NMR (qNMR) was first introduced as an analytical tool for quantitative
48 analysis in 1963 (Jungnickel and Forbes 1963). ¹H qNMR is the most widely used
49 technique for the quantitative measurement of multi-components in complex mixtures
50 without separation of the individual components (Bharti and Roy 2012). One of the
51 most used techniques in qNMR is to use an internal standard (Giraudeau et al. 2014).
52 That also removes the need to construct a calibration curve for the experiment. The
53 most important parameters for choosing the internal reference are its solubility, the
54 absence of chemical interactions and the similar relaxation times with the analytes and
55 a distinct chemical shift.

56 Hydrolysis reactions are an important class of reactions in food industry since invert
57 sugar, corn syrup, lactose-free milk are all produced through enzyme-catalyzed
58 reactions. Sucrose is a disaccharide composed of two monosaccharides which are
59 glucose and fructose. The hydrolysis of sucrose produces equal molar amounts of
60 glucose and fructose, forming a mixture which is called invert sugar (Figure 1). This
61 invert sugar is sweeter and less prone to crystallization compared to pure sucrose syrup
62 (Cotton et al. 1955). The resulting invert sugar is used in many applications such as
63 beverage and baking industry but most commonly to produce a soft fondant center in
64 confectionery (Edwards 2009). The production of invert sugar can be achieved either
65 with acid or enzymatic hydrolysis of sucrose. Although acid hydrolysis is used
66 traditionally, it has a low conversion efficiency, needs high energy consumption, causes
67 browning of the product and could result in the formation of carcinogenic by-products
68 like hydroxymethylfurfural (HMF) (Bailey 1966). A better method for producing invert

69 sugar is to use invertase enzyme resulting in higher yields with none of the
70 disadvantages of acid hydrolysis.

71 The competitive nature of process industry, especially food industry, requires to
72 produce high quality products with competitive prices and to adapt the process quickly
73 to changing customer needs. Many analytical methods are used in the food processing
74 industry. However, most of the traditional analytical methods are time-consuming and
75 sample-destructive. The use of quantitative online NMR spectroscopy is one such
76 promising alternative with its rapid and non-invasive properties. It can be easily
77 integrated to the process line in the factory with its high linearity feature between
78 absolute signal area and sample concentration.

79 In this study a method for the online monitoring of one of the most widely used
80 enzymatic reactions in food industry, sucrose hydrolysis, was tested by benchtop NMR
81 spectroscopy, and the method quantitative performance was evaluated.

82 **MATERIALS AND METHODS**

83 **Materials**

84 D-(+)-Glucose, D(-)-Fructose, Sucrose sugar and 3-(Trimethylsilyl) propionic-
85 2,2,3,3-d₄ acid (TSP) were provided from Sigma-Aldrich Co., St. Louis, MO, USA.
86 HPLC grade water from a water purification system (Nanopure Infinity, Barnstead
87 International, IA) was used for the preparation of the solutions. Acetic acid glacial from
88 VWR, Radnor, PA, USA was used for the pH adjustment. Invertase for the sucrose
89 hydrolysis was supplied from Sigma-Aldrich Co., St. Louis, MO, USA.

90

91

92 **Sample Preparations**

93 10% (w/w) glucose, fructose and sucrose solutions and their mixtures (Glucose +
94 Fructose+ Sucrose with a concentration of 10% (w/w)) were prepared separately by
95 dissolving in non-deuterated HPLC grade water in a 50 mL tube. During solution
96 preparation, 1% (w/w) TSP was added to all sugar solutions as the internal standard.
97 All solutions were stirred for 2 minutes for complete dissolution of sugars and TSP. pH
98 of the sugar solutions was adjusted to optimum working pH of the invertase enzyme
99 (pH=4.5) with glacial acetic acid. TSP with ^1H chemical shift of 4.810 ppm was chosen
100 as the chemical shift and concentration reference.

Commenté [PG2]: be careful!!

101 **NMR Experiments**

102 NMR experiments were performed on a low-field spectrometer operating at a 43 MHz
103 frequency with a compact permanent magnet based on the Halbach design (Magritek
104 Spinsolve, Wellington , NZ) (Danieli et al. 2010, 2013). This spectrometer is equipped
105 with a gradient coil along the transverse plane of the NMR tube that can produce a
106 maximum field gradient of 0.16 T.m^{-1} and also has an external lock system which
107 allows the use of non-deuterated solvents. For on-line monitoring, the system includes
108 a glass flow cell with 5 mm outer diameter, a peristaltic pump (Reglo Digital, Ismatec,
109 Wertheim, Germany) and PEEK tubing (Figure 2). The inner diameter of the flow cell
110 is 4 mm in the measurement region (10 mm in length) and decreases to 1 mm in upper
111 and lower regions of the measurement region to shorten the flow time during the
112 experiment. A heating plate (RCT Basic, IKA-Werke GmbH & Co. KG, Staufen,
113 Germany) was added to the system to control the temperature of the hydrolysis reaction.
114 The flow rate was also optimized as explained afterwards.

115

116 *Spin-Lattice Relaxation Time (T_1) Measurements*

117 An inversion recovery sequence was used for measuring longitudinal relaxation times
118 T_1 using an inversion time range, t of 0.1-10,000 ms with 15 points. The recovery curve
119 was fitted using Equation 1.

120
$$I = I_0(1 - 2 \cdot \exp\left(-\frac{t}{T_1}\right)) \quad (\text{Eq. 1})$$

121 *NMR Spectroscopy Experiments*

122 NMR experiments were carried out at 0.5 ml/min flow rate (see results and discussion
123 for optimization of this value). The experiments were performed at 29 °C since this
124 corresponds to the temperature at which the magnet stability is optimal. The
125 determination of appropriate solvent suppression pulse sequence was crucial while
126 working with non-deuterated solvents especially water. The gradient coil in the
127 spectrometer used enabled us to use recently developed solvent suppression methods
128 like the WET-180-NOESY pulse sequence (Gouilleux et al. 2017). This sequence gives
129 an optimal solvent suppression for small molecules on a benchtop spectrometer, leading
130 to a lower and narrower water signal with a clean phase with a minimal impact on
131 nearby peaks.

132 The Signal-to-Noise Ratios (SNR) were calculated using the SNR calculation script of
133 MestReNova software with 12.0.3 version (Mestrelab Research, Spain) by measuring
134 the height of the peaks of interest and dividing these values by the noise level. **The SNR**
135 **has been calculated and measured as 260 at the beginning of the experiments. During**
136 **the reaction, the C_6 concentration of sucrose decreased to 10 mg/g water starting from**
137 **60 mg/g-water. SNR at this concentration was calculated as 125. The limit of detection**
138 **was found as 4 mg/g -corresponding to an SNR of 10- water by extrapolation.** Here,
139 128 scans were found sufficient to yield an acceptable SNR for quantification. The 1D

140 ¹H spectra were obtained with 128 scans for a total experiment time of 12 min. The 90°
141 pulse angle was achieved by a pulse length of 6.7 μs at 0 dB. The FIDs were recorded
142 with 16 K points, a dwell time of 200 μs, and a repetition time of 6 s, corresponding to
143 5 times the longest T₁ (see below). The 1D data were processed with MestReNova
144 software. All spectra were processed with a 0.2 Hz exponential apodization, an
145 automatic phase correction and an automatic baseline correction via a Whittaker
146 smoother algorithm. **To align all the spectra correctly, TSP was used for ppm-scaling**
147 **reference and set at 0 ppm.** The resulting ¹H spectra from the different time points of
148 hydrolysis experiment were stacked too see the progress of hydrolysis.

149 *Quantitative Analysis*

150 For the quantitative NMR measurements, the glycosidic proton peak of sucrose and the
151 anomeric ~~proton~~carbon peak of glucose were chosen for hydrolysis follow up and for
152 the quantification. **Before peak integration, manual phase correction and manual**
153 **baseline correction were performed in addition to the automatic correction. This**
154 **procedure was found necessary to obtain a similar baseline for all the peaks that were**
155 **used for integration.** The resulting spectra from hydrolysis experiments were rearranged
156 as a superimposed plot. The integral areas of the internal reference (TSP), sucrose and
157 glucose were calculated by integration with the MestReNova software. Deconvolution
158 tools were also evaluated but yielded a slightly lower performance than integration,
159 probably due to the non-ideal line shapes. The integral areas of sucrose and glucose
160 were normalized according to the integral area of TSP. Concentrations of sucrose and
161 glucose for each time point were calculated using equation 2. The number of protons
162 contributing to the signal for TSP was taken as 9, for glucose and sucrose, it was taken
163 as 1.

Commenté [UW3]: This is also the anomeric 1H of sucrose ! replace glycosidic by anomeric

Commenté [UW4]: It is hard to detect 13C with a 1H/19F probehead ;)

164
$$C_x = \frac{A_x/N_x}{A_{TSP}/N_{TSP}} * \frac{MW_x}{MW_{TSP}} * C_{TSP} \quad (\text{Eq.2})$$

165 C , A , N , and MW are the concentration in mg/g, the integral area in a fully relaxed ^1H
166 NMR spectrum, the number of hydrogens contributing to the signals, and the molecular
167 weight. The x index refers to the analyte (sucrose or glucose) while the TSP index refers
168 to the internal reference.

169 **Kinetic Modelling**

170 The change of concentration of sucrose by time during hydrolysis was modelled using
171 a fractional conversion model kinetics equation (Equation 3) to find the rate constant.

172
$$\frac{C-C_\infty}{C_0-C_\infty} = e^{-kt} \quad (\text{Eq. 3})$$

173 C represents the concentration at time t , C_0 and C_∞ represents the initial and equilibrium
174 concentration respectively, and k represents the rate constant.

175

176 **RESULTS AND DISCUSSION**

177 *Exploring the 1D NMR Spectra*

178 1D NMR experiments were first conducted to identify the peaks which could be used
179 to monitor the sucrose hydrolysis reactions. Figure 3 shows the spectra of sucrose,
180 glucose and fructose solutions and the mixture of all sugars. Because of the relatively
181 low magnetic field, the resulting spectrum suffered from numerous overlaps between
182 3-4.5 ppm. The suppressed water peak can be seen at 4.9 ppm. Suppressing the water
183 signal is critical especially at low-field because overlapping issues become more
184 stringent due to the reduced spectral width at low frequency. Although the beta
185 anomeric proton of glucose is overlapped with the water peak, the alpha anomeric

186 proton of glucose is clearly seen at 5.3 ppm. In addition, the glycosidic proton of
187 sucrose at 5.48 ppm is very distinct. These two peaks can also be seen clearly in the
188 NMR spectrum of the mixture solution. Therefore, they were chosen to monitor the
189 hydrolysis of sucrose by the invertase enzyme.

190 *Determination of Optimal Flow Rate*

191 The choice of the optimal flow rate is one of the critical parameters in flow NMR
192 experiments as the signal becomes broader and the resolution decreases with increasing
193 flow rates. In flow NMR, 'inflow' and 'outflow' effects need to be considered carefully.
194 During the experiment, the excited spins in the sensitive volume are refreshed by
195 unexcited ones, leading to shorter apparent T_1 . This 'inflow' effect allows shorter
196 repetition times (T_R) to reach quantitative conditions (Nordon et al. 2001). But when
197 the flow rate is significantly high, excited spins leave the sensitive volume before the
198 acquisition of the FID is finished. This is called 'outflow' effect. This causes severe
199 line broadening and affects the resolution of the NMR spectra (Gouilleux et al. 2017).
200 To determine the optimum flow rate to be used in hydrolysis experiments, NMR spectra
201 of the model mixture were recorded in non-flow conditions and in flow with 0.5 ml/min,
202 1 ml/min and 2 ml/min flow rates. As observed in Figure 4, when the flow rate increases
203 from 0 ml/min to 2 ml/min, the peaks became broader and the glucose peak overlapped
204 with the water peak, as a consequence of the outflow effect. Therefore, it was decided
205 to use 0.5 ml/min flow rate in the online monitoring of hydrolysis reactions, which
206 resulted in a modest reduction of longitudinal relaxation times (see below) resulting
207 from the inflow effect.

208 *Spin-Lattice Relaxation Time (T_1) and Repetition Time (T_R) Measurements*

209 As stated before, spin-lattice relaxation times (T_1) were measured by the Inversion

210 Recovery pulse sequence. For quantitative measurements, the peak of interest with the
211 longest T_1 is the limiting factor, in our case TSP. For the corresponding peak, T_1 values
212 were measured as 1.2, 1.1, 0.97 and 0.93 s in non-flow and in flow conditions with the
213 flow rates of 0.5 ml/min, 1 ml/min and 2 ml/min, respectively. Here, the choice of a 0.5
214 ml/min flow rate resulted in a negligible reduction of the relaxation time, but was
215 necessary to avoid significant broadening (see above). In order to ensure a 1% accuracy
216 on the quantitative measurements, the repetition time TR was set to about 5 times the
217 longest T_1 , leading to TR = 6 s.

218 **Online Monitoring and Kinetic Modelling of Sucrose Hydrolysis with qNMR**

219 **Measurements**

220 In Figure 5, the consumption of sucrose and the production of glucose in the course of
221 the hydrolysis are clearly observable. At time around 240 min, the integral area of
222 sucrose reaches to a constant value and does not change after this time.

223 Hydrolysis experiments were repeated 3 times and the change of the mean
224 concentrations of sucrose and glucose as a function of time can be seen in Figure 6,
225 showing the good repeatability of the experiments. In this figure, it is seen that 1/6 of
226 the sucrose ~~not being~~ was not converted. This might have been caused by invertase
227 optimum temperature and substrate inhibition. The optimum temperature for the
228 activity of invertase is between 50 °C -60 °C. However, the experiments were
229 performed at 29 °C because this corresponds to the temperature at which the magnet
230 stability is optimal. This may affect the reaction rate and the amount sucrose converted.
231 Also, the activity of invertase is affected by the substrate concentration. The maximum
232 rate of hydrolysis is obtained with a sucrose concentration of 5 to 10%, and then with
233 higher concentrations, the rate decreases (Bergmeyer, 1965). In the experiments, 10%

234 sucrose concentration has been used and this may affect the amount of sucrose being
235 converted.

236 The mean concentrations of TSP were also plotted as a function of time to demonstrate
237 baseline variation of the experiments (Figure 7). The mean curve was plotted for
238 sucrose concentration and the data were fitted by equation 3. The average rate constant
239 was found as $k = [12.88 \pm 1.96] \times 10^{-3} \text{ min}^{-1}$ (Figure 8) at 29°C. Vu and Le (2008)
240 studied the kinetics of the immobilized and free invertase and found the kinetic constant
241 for free invertase as $1.8 \times 10^{-3} \text{ min}^{-1}$, $4.1 \times 10^{-3} \text{ min}^{-1}$, $3.2 \times 10^{-2} \text{ min}^{-1}$ at 50°C, 55°C,
242 60°C respectively (Vu and Le 2008). In the aforementioned study, although a different
243 approach (a new enzyme-catalyzed reaction was performed every time to see
244 how the activity changed with respect to the initial enzyme-catalyzed reaction) was
245 followed to calculate the activity of the enzyme, in terms of order of magnitude, values
246 were found to be reasonably close to the ones obtained in this study ($\sim 10^{-3}$). The
247 differences might have been caused by the temperature, the initial concentration or the
248 activity of the enzyme used in this study.

249

250

251

252

253

254

255

256

257 **CONCLUSION**

258 This study shows that benchtop quantitative ¹H NMR is a relatively easy and rapid
259 method for the online monitoring and quantification of enzymatic reactions, which can
260 easily be implemented for a variety of food chemistry applications and it could play a
261 central role in the control of production processes in food industry.

262 Although not performed here, since it is now shown that such reactions can easily be
263 monitored with this technique, as a further study the reaction parameters ~~can~~ could be
264 changed and Michaelis Menten kinetic analysis could be conducted to find the kinetic
265 parameters.

266 **Compliance with Ethical Standards**

267 **Funding:** Alper Soyler got funding from Short Term Scientific Mission (STSM)
268 program under COST Action CA15209 EURELAX – European Network on NMR
269 Relaxometry (http://www.cost.eu/COST_Actions/ca/CA15209) to conduct
270 experiments at the University of Nantes. Authors from Nantes acknowledge support
271 from the Corsaire metabolomics core facility (Biogenouest).

272 **Conflict of Interest:** Alper Soyler declares that he has no conflict of interest. Dylan
273 Bouillaud declares that he has no conflict of interest. Jonathan Farjon declares that he
274 has no conflict of interest. Patrick Giraudeau declares that he has no conflict of interest.
275 Mecit H. Oztop declares that he has no conflict of interest

276 **Ethical Approval:** This article does not contain any studies with human or animal
277 subjects.

278 **Informed Consent:** Publication has been approved by all individual participants.

279

Commenté [PG5]: why not writing that all the authors declare that they have no conflict of interest?

280

281 **REFERENCES**

282 Bailey L (1966) The effect of acid-hydrolysed sucrose on honeybees. *J Apic Res.* doi:

283 10.1080/00218839.1966.11100146

284 Bergmeyer H.U. (1965) *Methods of Enzymatic Analysis*. Academic Press, pp 901-

285 907

286 Bharti SK, Roy R (2012) Quantitative ¹H NMR spectroscopy. *TrAC - Trends Anal.*

287 *Chem.*

288 Blümich B, Singh K (2018) *Desktop NMR and Its Applications From Materials*

289 *Science To Organic Chemistry*. *Angew. Chemie - Int. Ed.*

290 Chen FL, Wei YM, Zhang B (2010) Characterization of water state and distribution in

291 textured soybean protein using DSC and NMR. *J Food Eng.* doi:

292 10.1016/j.jfoodeng.2010.04.040

293 Cotton RH, Rebers PA, Maudru JE, H GUYRG (1955) The Role of Sugar in the Food

294 Industry. 3–20

295 Dalitz F, Cudaj M, Maiwald M, Guthausen G (2012) Process and reaction monitoring

296 by low-field NMR spectroscopy. *Prog. Nucl. Magn. Reson. Spectrosc.*

297 Danieli E, Perlo J, Blümich B, Casanova F (2013) Highly stable and finely tuned

298 magnetic fields generated by permanent magnet assemblies. *Phys Rev Lett.* doi:

299 10.1103/PhysRevLett.110.180801

300 Danieli E, Perlo J, Blümich B, Casanova F (2010) Small magnets for portable NMR

301 spectrometers. *Angew Chemie - Int Ed.* doi: 10.1002/anie.201000221

302 Edwards WP (Bill) (2009) Caramels, fondants and jellies as centres and fillings. In:
303 Science and Technology of Enrobed and Filled Chocolate, Confectionery and
304 Bakery Products. Elsevier, pp 123–151

305 Giraudeau P, Tea I, Remaud GS, Akoka S (2014), Reference and normalization
306 methods: Essential tools for the intercomparison of NMR spectra. *Journal of*
307 *Pharmaceutical and Biomedical Analysis*, 93, 3-16

308 Gouilleux B, Charrier B, Akoka S, Giraudeau P (2017) Gradient-based solvent
309 suppression methods on a benchtop spectrometer. *Magn Reson Chem*. doi:
310 10.1002/mrc.4493

311 Gouilleux B, Marchand J, Charrier B, et al (2018) High-throughput authentication of
312 edible oils with benchtop Ultrafast 2D NMR. *Food Chem*. doi:
313 10.1016/j.foodchem.2017.10.016

314 Hu Y, Wang S, Wang S, Lu X (2017) Application of nuclear magnetic resonance
315 spectroscopy in food adulteration determination: The example of Sudan dye i in
316 paprika powder. *Sci Rep*. doi: 10.1038/s41598-017-02921-8

317 Jungnickel JL, Forbes JW (1963) Quantitative Measurement of Hydrogen Types by
318 Integrated Nuclear Magnetic Resonance Intensities. *Anal Chem*. doi:
319 10.1021/ac60201a005

320 Keeton JT, Hafley BS, Eddy SM, et al (2003) Rapid determination of moisture and fat
321 in meats by microwave and nuclear magnetic resonance analysis--PVM 1:2003. *J*
322 *AOAC Int*. doi: 10.1017/CBO9781107415324.004

323 Kumar D, Singh B, Baudhdh K, Korstad J (2015) Bio-oil and Biodiesel as Biofuels
324 Derived from Microalgal Oil and Their Characterization by Using Instrumental

325 Techniques. In: *Algae and Environmental Sustainability*. Springer India, New
326 Delhi, pp 87–95

327 Marcone MF, Wang S, Albabish W, et al (2013) Diverse food-based applications of
328 nuclear magnetic resonance (NMR) technology. *FRIN* 51:729–747. doi:
329 10.1016/j.foodres.2012.12.046

330 Meyer K, Kern S, Zientek N, et al (2016) Process control with compact NMR. *TrAC -*
331 *Trends Anal. Chem.*

332 Nestor G, Bankefors J, Schlechtriem C, et al (2010) High-resolution ¹H magic angle
333 spinning nmr spectroscopy of intact arctic char (*Salvelinus Alpinus*) muscle.
334 quantitative analysis of n-3 fatty acids, EPA and DHA. *J Agric Food Chem.* doi:
335 10.1021/jf103338j

336 Nordon A, McGill CA, Littlejohn D (2001) Process NMR spectrometry. *Analyst*

337 Pentimalli M, Capitani D, Ferrando A, et al (2000) Gamma irradiation of food
338 packaging materials: An NMR study. *Polymer (Guildf)*. doi: 10.1016/S0032-
339 3861(99)00473-5

340 Picone G, Mezzetti B, Babini E, et al (2011) Unsupervised principal component
341 analysis of NMR metabolic profiles for the assessment of substantial equivalence
342 of transgenic grapes (*vitis vinifera*). *J Agric Food Chem.* doi: 10.1021/jf2020717

343 Vu TKH, Le VVM (2008) Biochemical studies on the immobilization of the enzyme
344 invertase (EC.3.2.1.26) in alginate gel and its kinetics. *Int Food Res J* 15:73–78

345

346

347

348 **FIGURE CAPTIONS**

349 **Figure 1.** Hydrolysis of sucrose into glucose and fructose.

350 **Figure 2.** System setup for online reaction monitoring

351 **Figure 3.** 1D ^1H NMR spectra of sucrose solution, glucose solution, fructose solution
352 and mixture of all sugars recorded at 43 MHz with water signal suppression.

353 **Figure 4.** 1D ^1H NMR spectra of model mixture solution recorded at 43 MHz in
354 different flow rates of 0 ml/min, 0.5 ml/min, 1.0 ml/min, 2 ml/min, with water signal
355 suppression.

356 **Figure 5.** 1D ^1H NMR spectra of sucrose hydrolysis recorded at 43 MHz.

357 **Figure 6.** Sucrose and glucose concentration changes in the course of sucrose
358 hydrolysis by invertase, monitored by quantitative ^1H NMR benchtop spectroscopy.
359 Error bars are standard deviations calculated on 3 successive experiments performed in
360 the same conditions.

361 **Figure 7.** The mean concentration changes of TSP as a function of time. Error bars are
362 standard deviations calculated on 3 successive experiments performed in the same
363 conditions.

364 **Figure 8.** First order reaction kinetics obtained by adjusting the time evolution of
365 sucrose concentration by a fractional conversion model.

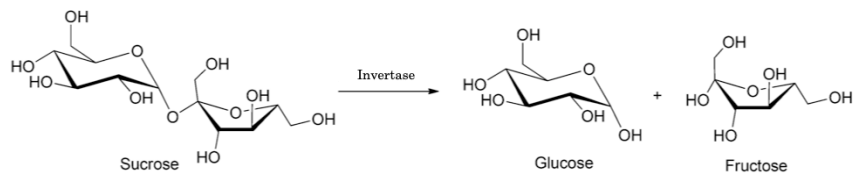
366

367

368

369

370



371

372 **Figure 1**

373

374

375

376

377

378

379

380

381

382

383

384

385

386

387

388



389

390 **Figure 2**

391

392

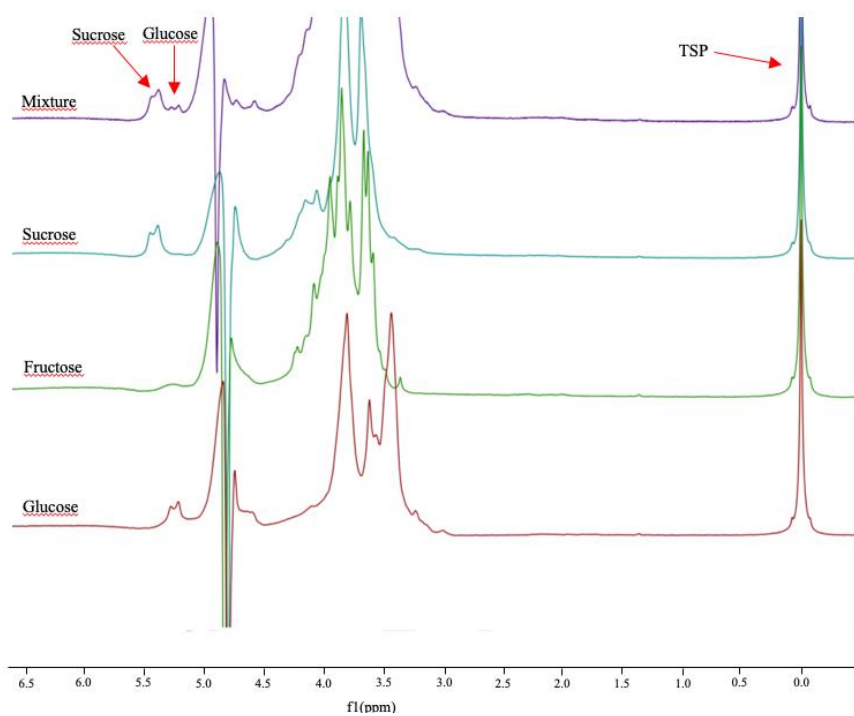
393

394

395

396

397



398

399 **Figure 3**

400

401

402

403

404

405

406

407

408

409

410

411

412

413

414

415

416

417

418

419 **Figure 4**

420

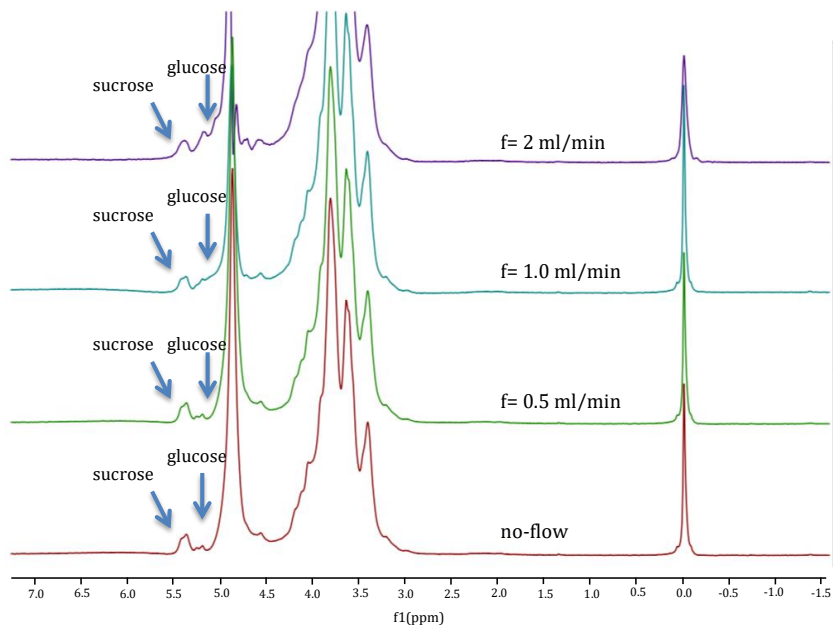
421

422

423

424

425



426

427

428

429

430

431

432

433

434

435

436

437

438

439

440

441

442

443

444

445

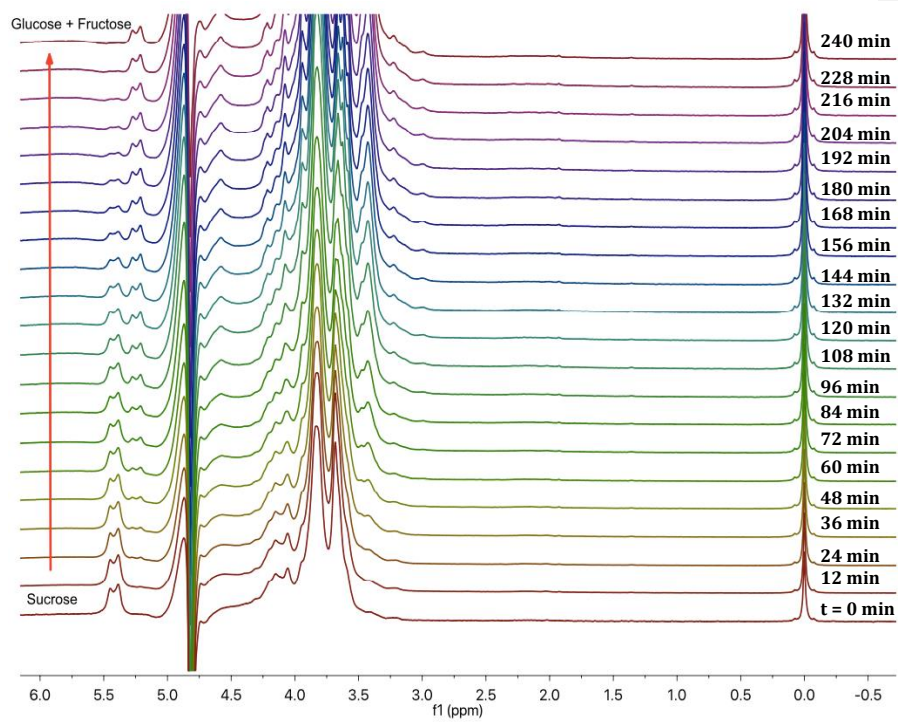
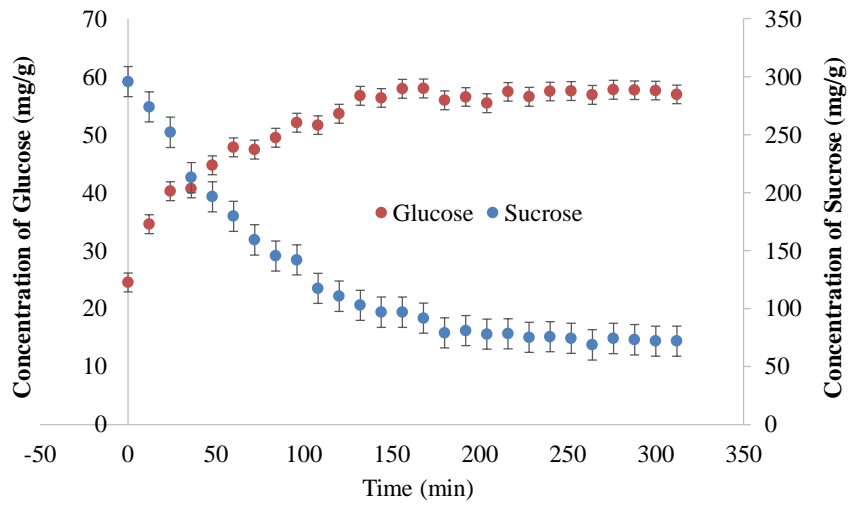


Figure 5

446

447



448

449 **Figure 6**

450

451

452

453

454

455

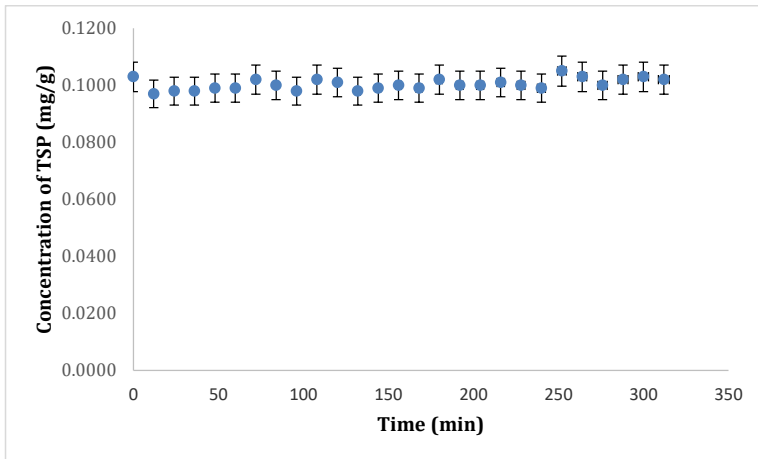
456

457

458

459

460



461

462

463 **Figure 7**

464

465

466

467

468

469

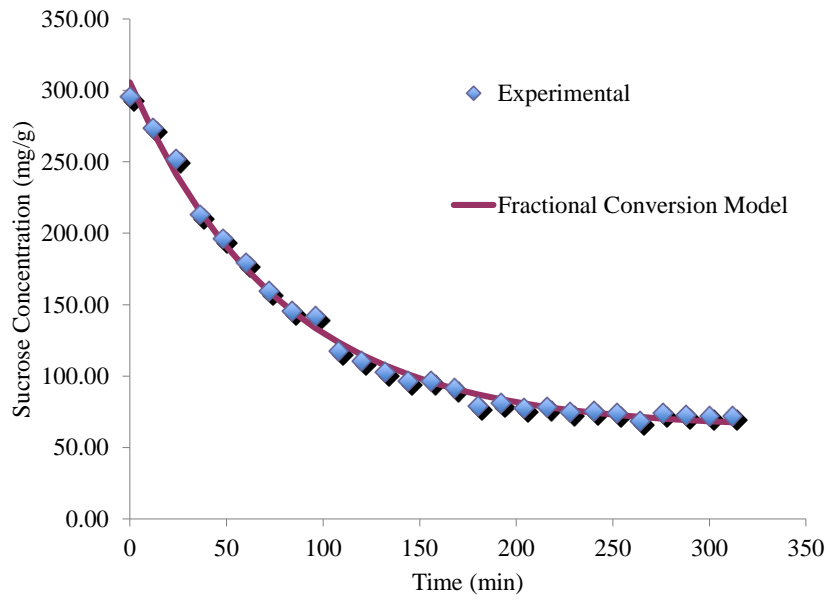
470

471

472

473

474



475

476 **Figure 8**

477